Piotr SOBAŃSKI

Wroclaw University of Technology, Institute of Electrical Machines, Drives and Measurements

Fuzzy-logic-based approach to voltage inverter fault diagnosis in induction motor drive

***Abstract**. In this paper simulation results of a single IGBT open-circuit fault diagnostic system for a two-level voltage inverter-fed direct field-oriented controlled induction motor drive are presented. A fault diagnostic procedure is carried out by utilizing an analysis of an estimated rotor flux space vector trajectory in stationary α–β coordinates. In the article an original approach for a fault extraction procedure based on fuzzy-logic system with on-line membership functions parameter adjustment in a fuzzification layer is proposed.*

***Streszczenie.** W artykule zaprezentowano wyniki badań symulacyjnych systemu diagnostyki uszkodzeń polegających na braku przewodzenia prądu przez jeden z tranzystorów IGBT dwupoziomowego falownika napięcia w napędzie indukcyjnym z bezpośrednim sterowaniem polowo zorientowanym. Metoda diagnostyki awarii została oparta na analizie przebiegu wektora estymowanego strumienia wirnika w układzie współrzędnych stacjonarnych α-β. W pracy przedstawiono oryginalny sposób ekstrakcji symptomów uszkodzeń, który polega na zastosowaniu zbiorów rozmytych o przestrajalnych parametrach funkcji przynależności w warstwie rozmywania. (**Zastosowanie logiki rozmytej do diagnostyki uszkodzeń falownika napięcia w napędzie indukcyjnym**).*

Keywords: fuzzy logic, induction motor, voltage inverter, IGBT fault diagnosis.
Słowa kluczowe: logika rozmyta, silnik indukcyjny, falownik napięcia, diagnostyka uszkodzeń tranzystorów IGBT.

doi:10.12915/pe.2014.06.28

Introduction

Due to a wide development of power electronic converters, squirrel-cage induction machines are currently the most commonly used AC motors in industrial drive applications. In spite of a high reliability of an induction machine construction, electrical drives based on squirrel-cage motors suffer several faults. Over half of AC drive failures are related to disturbances of power semiconductor devices, namely short- and open-circuit faults [1]. Typically, short-circuit protection methods rely on additional hardware application, such as a fast fuse in a DC-link of a power converter. Unfortunately, turning on the fuse brings on shutdown a motor. A modern inverter short-circuit protection scheme is based on high integrated transistor drivers, in many cases turning off an affected transistor before its permanent damage. Indeed, a drive performance is significantly reduced after turning off the switch, but a high current doesn't flow though a converter and therefore further rapidly progressive inverter faults can be avoided. On the other hand, open-transistor failures can be caused by optocoupler or driver transistor failures, as well as may result from transistor's gate junction dysfunctions [2]. A high quality drive performance can be maintained even under inverter faulty operations, providing that a faulty semiconductor device is recognized and a remedial action for a converter is carried out as fast as possible. Moreover, if a time duration of the fault diagnosis is reduced, the post-fault action will be undertaken faster and therefore a possibility of further faults will be minimized.

Open-switch faults diagnosis methods for inverter-fed motor drive systems can be divided into voltage- and current-based techniques. An additional sensors application for an inverter's voltage measurements is the most effective way to achieve a great effectiveness of a transistor fault diagnosis in electrical drives. In papers [3]-[6], the open-switch fault diagnosis methods based on a comparison between measured inverter voltages and their expected references are described. Despite of experimentally proof of these techniques, their industrial application is rather limited due to an extra sensors utilisation requirement, which increases a drive implementation cost. Therefore, diagnostic algorithms based on an analysis of state variables, that are calculated by using normally measured signals for a vector drive control, namely stator currents, DC-link voltage and angular rotor speed have been extensively investigated recently. As an example, an open-switch fault diagnostic technique presented in [7] utilizes average values of errors between reference and estimated voltages that can be calculated from a current-based flux estimator. Another approach to an open-switch fault diagnosis in a voltage inverter is based on stator currents analysis. As an example, there are many inverter fault diagnosis techniques, which main idea relies on comparison between a stator current vector hodograph functions under healthy and faulty drive operations [8]. These algorithms were comprehensively described in paper [9]. Unlike the voltage sensor-based diagnostic methods, to carry out a diagnosis procedure, the current-based techniques demand more time than one current period in many cases. While a faulty transistor identification is carried out, a risk of an unexpected motor stall is increased, in particular under low-speed and full-load torque drive operations.

In this paper an original approach to an open-circuit faults diagnosis in a two-level three-phase voltage inverter-fed induction motor drive is presented. The proposed method is based on an analysis of the estimated rotor flux vector in stationary α-β reference frames. Additionally, the fast and effective diagnosis is achieved due to an on-line fuzzy system parameters adjustment. Furthermore, to realize the diagnostic procedure, no extra sensors are required. Presented results were achieved by a simulation model of the direct rotor field-oriented controlled (*DRFOC*) induction motor drive system.

Inverter faults diagnostic method

A motor supply voltage asymmetry, which is related to an open-switch fault of the two-level voltage inverter (see Fig. 1), disturbs controlled drive state variables, including an amplitude of an estimated rotor flux vector $\hat{\psi}_r$ [10]. The rotor flux estimation, which is essential for the Direct Rotor Field Oriented Control (*DRFOC*), can be obtained using simple simulators or more complex structures, such as state observers [9]. So a stator equation-based rotor-flux-simulator or a state observer, e.g. the Luenberger observer can be utilized. In both cases, stator phase currents are measured and stator phase voltages $u_{sA,B,C}$ should be calculated by using simple relations between transistor state reference signals $S_{A,B,C}$ and the inverter DC-link voltage U_{DC} in accordance with (1)-(3) [11]:

(1) $$\hat{u}_{sA} = \frac{U_{DC}}{3}\left(2S_A - S_B - S_C\right)$$

(2) $$\hat{u}_{sB} = \frac{U_{DC}}{3}\left(2S_B - S_A - S_C\right)$$

(3) $$\hat{u}_{sC} = \frac{U_{DC}}{3}\left(2S_C - S_B - S_A\right)$$

where: $\hat{u}_{sA}, \hat{u}_{sB}, \hat{u}_{sC}$ - estimated stator voltages.

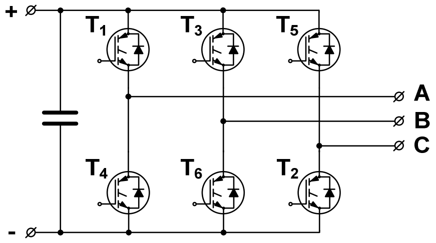

Fig.1. Two-level three-phase voltage inverter topology

It is noticeable that the voltages $\hat{u}_{sA}, \hat{u}_{sB}, \hat{u}_{sC}$ cannot be calculated correctly in case of any transistor faults. As an example, if transistor T_1 is affected and S_A=1, it is impossible to obtain reference inverter voltages. In spite of this fact, the rotor flux cannot be estimated properly. This drawback can be avoided using the inverter voltage measurements instead of their estimated values. Nevertheless, this solution significantly increase a drive implementation cost. On the other hand, assuming that normalized motor parameters, namely: rotor resistance, rotor leakage and mutual reactances are constant, the current-based flux simulator [12], that is a function of normalized stator currents $i_{sA,B,C}$ and a normalized angular motor speed ω_m, is not affected by false information related to the stator voltages (see Eq. (4) and (5)):

(4) $$\hat{\psi}_{r\alpha} = \frac{1}{T_N}\int\left[\frac{r_r}{x_r}\left(x_M i_{s\alpha} - \hat{\psi}_{r\alpha}\right) - \omega_m \hat{\psi}_{r\beta}\right]dt$$

(5) $$\hat{\psi}_{r\beta} = \frac{1}{T_N}\int\left[\frac{r_r}{x_r}\left(x_M i_{s\beta} - \hat{\psi}_{r\beta}\right) + \omega_m \hat{\psi}_{r\alpha}\right]dt$$

where: $T_N = \frac{1}{2\pi f_{sN}}$, f_{sN} - nominal stator voltage frequency.

Assuming a symmetric machine and a healthy drive operation, stator phase currents can be described in accordance with (6):

(6) $$i_{sf} = \begin{cases} i_{sA} = I_{mf}\sin\left(2\pi ft + \varphi\right) \\ i_{sB} = I_{mf}\sin\left(2\pi ft - \frac{2\pi}{3} + \varphi\right) \\ i_{sC} = I_{mf}\sin\left(2\pi ft + \frac{2\pi}{3} + \varphi\right) \end{cases}$$

where: I_{mf} - current amplitude, f - current frequency, t - time, φ - initial phase angle.

If the inverter open-switch fault occurs, an unidirectional current flow in an affected motor phase is observed. As an example, if transistor T_1 is permanently turned-off, assuming φ=0, the i_{sA} current can be described as a function (7):

(7) $$i_{sA} = \begin{cases} 0 \quad dla\, 0 < t < \frac{1}{2f} \\ I_{mf}\sin\left(2\pi f\right) \quad \frac{1}{2f} < t < \frac{1}{f} \end{cases}$$

Applying the Clark transformation to the equation (6) yields the following equations in the stationary α–β frame (8):

(8) $$\begin{aligned} i_{s\alpha} &= \frac{2}{3}\left(i_{sA} - \frac{1}{2}i_{sB} - \frac{1}{2}i_{sC}\right) \\ i_{s\beta} &= \frac{2}{3}\left(\frac{\sqrt{3}}{2}i_{sA} + \sqrt{3}i_{sB}\right) \end{aligned}$$

Transforming the formulas (4)-(5) by substitution the equation (7) and (8), shows that the T_1 fault affects $\hat{\psi}_{r\alpha}$ and $\hat{\psi}_{r\beta}$ as well. Since the rotor flux α–β components are coupled (4)-(5), the transistor fault diagnostic algorithm is more complicated. To extract open-switch fault features the equations (4)-(5) can be written in the polar coordinates, in accordance with relations (9)-(10):

(9) $$\hat{\psi}_r = \sqrt{\hat{\psi}_{r\alpha}^2 + \hat{\psi}_{r\beta}^2}$$

(10) $$\gamma = arctan\left(\frac{\hat{\psi}_{r\beta}}{\hat{\psi}_{r\alpha}}\right)$$

where: γ - angle defines rotor flux position in the α–β frame.

During a healthy inverter mode it can be assumed, that in case of the *DRFOC* drive the estimated rotor flux modulus $\hat{\psi}_r$ is approximately constant and equal to the reference, nominal value. As a result of an asymmetrical power supply, which is related to the open-transistor faults, once a period of the rotor flux vector rotational movement, the absolute value of the estimated rotor flux significantly increases above and once decreases under the nominal value $\psi_{r\,ref}$. In accordance with the proposed inverter faults diagnosis method, the absolute value of the estimated rotor flux vector and its phase γ is analyzed simultaneously in stationary α–β reference frame. Additionally, in order to determine a faulty transistor, a value of an angle γ_v related to the local minimum of $\hat{\psi}_r$ and γ_h connected to the local maximum of $\hat{\psi}_r$ is stored. For any transistor faults, characteristic ranges of the γ_v and γ_h can be specified, nevertheless to achieve a good diagnostic method, effectiveness a drive working conditions have to be taken into consideration. A value $\omega_{v,h}$ of the angular motor speed ω_m, that is related to a moment of a rotor flux local extremum, is utilized to the diagnosis system adjustment.

A block diagram of the diagnostic system is shown in Fig. 2 In accordance with the sequential system scheme, during normal drive operation only a first part of the system is activated. In that part, a changing dynamics of the signal $\hat{\psi}_r$ is reduced by using low-pass filter with cut-off frequency 1kHz. Additionally, local extreme value of the $\hat{\psi}_r$ is identified and γ_v or γ_h and $\hat{\psi}_r$ are stored. Furthermore, depending on the extrema type (a local minimum or a local maximum) the angular speed value ω_v or ω_h is accumulated as well. Farther, a previously stored value of the $\hat{\psi}_r$ is compared with a fault threshold value that is generated by a function $\psi_{r\,min}(|\omega_m|)$ in case of a local minimum detection or $\psi_{r\,max}(|\omega_m|)$=const, in case of a local maximum identification. If the fault threshold is reached, the second part of the diagnostic system is activated. The functions: $\psi_{r\,min}(|\omega_m|)$ and $\psi_{r\,max}(|\omega_m|)$ were designed by simulations, so that the fault thresholds are not achieved during a healthy drive operation.

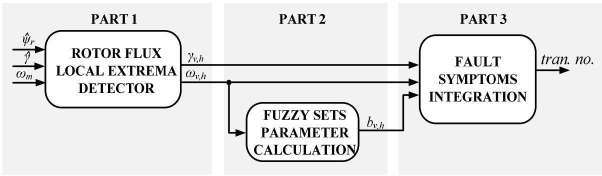

Fig.2. Sequential diagnostic system scheme

To simplify a design process of the function $\psi_{r\,min}(|\omega_m|)$, a fuzzy-logic-based approach was applied. Shape and distribution of membership functions $A_j : j \in \{1,\ldots,6\}$ utilized for the $\psi_{r\,min}(|\omega_m|)$ approximation are presented in Fig. 3.

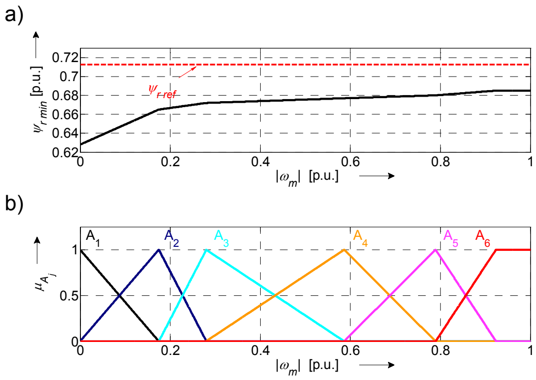

Fig.3. Function $\psi_{r\,min}(|\omega_m|)$ (a) and membership functions A_j (b)

Depending on the identified extrema type of $\hat{\psi}_r$, each domain of the functions $C_k : k \in \{1,\ldots,8\}$, which are related to the third stage of the diagnostic algorithm, is calculated according to the ω_v or ω_h and parameters: b_v or b_h that are calculated in the second part of the diagnostic system (see Fig. 2). The shape of the particular membership functions C_k is always the same and their distribution is regular but the domains of the functions is slightly changeable (see Fig. 4). Depending on a value and motor speed direction, all membership functions C_k are translated by a vector $\vec{u} = \lfloor b_{v,h}, 0 \rfloor$, that means $\mu_{Ck}(\gamma_{v,h}) \xrightarrow{\vec{u}} \mu_{Ck}(\gamma_{v,h} - b_{v,h})$, where b_v=f(ω_v) and b_h=f(ω_h) are described by the following expressions (12)-(13):

$$b_v(\omega_v) = \begin{cases} \omega_v > 0 & g_1\omega_v + g_2 \\ \omega_v \le 0 & -g_1\omega_v - g_2 \end{cases} \quad (12)$$

$$b_h(\omega_h) = \begin{cases} \omega_h > 0 & g_3\omega_h + g_4 \\ \omega_h \le 0 & -g_3\omega_h - g_4 \end{cases}$$

where: g_1=0, g_2=-1,360e-002, g_3=3,500e-004, g_4=-1,400e-001,

$$\begin{aligned} &\omega_v > 0 \Rightarrow b_v \in \langle -0{,}07, 0{,}35 \rangle \; or \\ &\omega_v < 0 \Rightarrow b_v \in \langle -0{,}35, 0{,}07 \rangle \; or \\ &\omega_h > 0 \Rightarrow b_h \in \langle -0{,}01, 0{,}025 \rangle \; or \\ &\omega_h < 0 \Rightarrow b_h \in \langle -0{,}025, 0{,}01 \rangle \end{aligned} \quad (13)$$

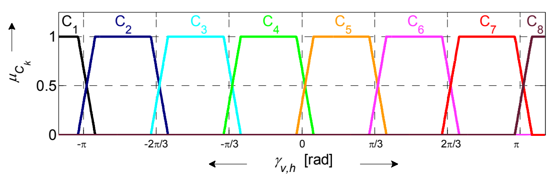

Fig.4. Exemplary distribution of the membership functions C_k

In accordance with Fig. 5, the α–β plane was divided into six sectors that are specified by ranges of the angle $\gamma_{v,h}$. Points $C_{1cen},\ldots,C_{6cen}$ are related to median of each function C_k domain. Additionally, arrows show the influence of the $b_{v,h}$ on $C_{1cen},\ldots,C_{6cen}$ distribution. For a further diagnostic technique explanation, basic rules of the proposed diagnosis method are shown in the Table 1.

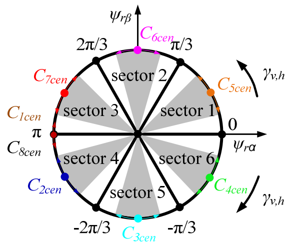

Fig.5. Relationship between sectors of the α–β plane and C_k functions

Table 1. Patterns of the open-switch fault symptoms

Character of $\omega_{v,h}$	Extremum	Sector number					
		1	2	3	4	5	6
ω_v>0	min. ($\hat{\psi}_r$)	T_1	T_2	T_3	T_4	T_5	T_6
ω_h>0	max. ($\hat{\psi}_r$)	T_6	T_1	T_2	T_3	T_4	T_5
ω_v≤0	min. ($\hat{\psi}_r$)	T_2	T_3	T_4	T_5	T_6	T_1
ω_h≤0	max. ($\hat{\psi}_r$)	T_3	T_4	T_5	T_6	T_1	T_2

As an example, if a local minimum of $\hat{\psi}_r$ is detected and then ω_v as well as γ_v are stored, degrees of membership of γ_v to the fuzzy sets, that are described by functions C_k, are calculated. The membership functions C_k are strictly related to the α–β plane sectors, so that a faulty transistor can be identified by applying rules formulated in the Table 1. For example, if T_1 transistor is faulty and the angular drive speed is positive, depending on an identified extremum of $\hat{\psi}_r$, a degree of membership of γ_v to the fuzzy set, which is defined by the function C_5 related to the sector 1, is the highest. The same applies to the local maximum of $\hat{\psi}_r$, a degree of membership of γ_v to the fuzzy set, that is defined by the function C_4 related to the sector 6, is the highest.

A block diagram of the third part of the transistor fault diagnosis system is shown in Fig. 6.

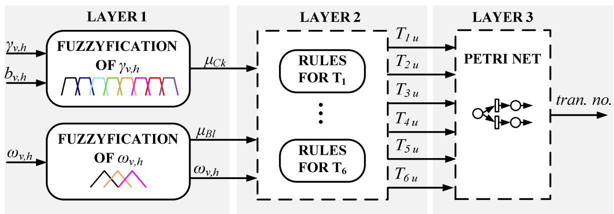

Fig.6. Block diagram of the fault symptoms integration stage of the diagnostic procedure

For the inference process, which is carried out in the second layer of the third diagnostic system part (see Fig. 6), a modulus of the speed $|\omega_{v,h}|$ is analyzed by using fuzzy logic membership functions $B_j : j \in \{1,\ldots,3\}$ that shape and distribution is shown in Fig. 7.

Depending on a motor speed direction and a degree of membership of $|\omega_{v,h}|$ to the fuzzy sets, that are described by functions B_j, appropriate rules containing sets are chosen. As an example, the open-circuit transistor T_1 diagnostic rule base is described by the Table 2 and the Table 3.

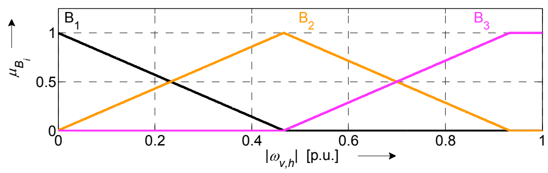

Fig.7. Shape and distribution of the membership functions B_j

Table 2. Diagnostic rulebase for faulty transistor T_1 in case of the local minimum of $\hat{\psi}_r$ appearance

	$\omega_m>0$							
	C_1	C_2	C_3	C_4	C_5	C_6	C_7	C_8
B_1	0	0	0	0,6	1	0	0	0
B_2	0	0	0	0	1	0	0	0
B_3	0	0	0	0	1	0,6	0	0
	$\omega_m\leq 0$							
	C_1	C_2	C_3	C_4	C_5	C_6	C_7	C_8
B_1	0	0	0	1	0,6	0	0	0
B_2	0	0	0	1	0	0	0	0
B_3	0	0	0,6	1	0	0	0	0

Table 3. Diagnostic rulebase for faulty transistor T_1 in case of the local maximum of $\hat{\psi}_r$ appearance

	$\omega_m>0$							
	C_1	C_2	C_3	C_4	C_5	C_6	C_7	C_8
B_1	0	0	0	0	0,6	1	0	0
B_2	0	0	0	0	0	1	0	0
B_3	0	0	0	0	0	1	0,6	0
	$\omega_m\leq 0$							
	C_1	C_2	C_3	C_4	C_5	C_6	C_7	C_8
B_1	0	0	1	0,6	0	0	0	0
B_2	0	0	1	0	0	0	0	0
B_3	0	0,6	1	0	0	0	0	0

For a defuzzification process, a singleton method was applied. Output signals $T_{1u},\ldots,T_{6u}$ of the second layer are strictly related to each transistor condition monitoring subsystem, respectively T_{1u} signal corresponds to transistor T_1, T_{2u} is related to T_2, etc. To decide, which transistor is faulty, competitive Petri net, that finds the maximal signal of the second layer, is introduced.

Simulation results

The effectiveness of the diagnostic method was confirmed by simulation model of the *DRFOC* induction motor drive designed in MATLAB/Simulink. In accordance to the drive model, the 1.1 kW three-phase motor is fed by two-level voltage inverter. The power converter was modeled using SimPower System toolbox, which allowed simple open-switch fault simulations by permanently applying 0 logic signal on transistor gates [9].

For each transistor, the open-circuit faults were simulated under various drive condition (see Fig. 8, 9.). Round, cyan markers refer to registered values of the γ_v and γ_h during no-load drive operation m_l=0. Triangular, green markers correspond to load m_l=0,5m_N and rectangular, orange ones concern the full-load drive operation m_l=m_N. The transistor fault simulations refer to a drive speed range $\omega_m \in \langle 0.3\omega_N, \omega_N \rangle$ and $\omega_m \in \langle -0.3\omega_N, -\omega_N \rangle$, where ω_N means a nominal angular rotor speed. Additionally, arrows show a direction of growth of the angular motor speed ω_m. The inverter fault diagnostic rules (Tab. 1.) were formulated on grounds of the simulation results shown in Fig. 8 and Fig. 9. During a drive operation at a medium angular speed ω_m≈0,5ω_N, a faulty transistor can be identified only by knowing the angle γ_v or γ_h. As can be seen, in range of low or near the nominal motor speed, to avoid false diagnosis, a value of the $\omega_{v,h}$ speed, that is related to the local extremum of $\hat{\psi}_r$ occurrence, is necessary.

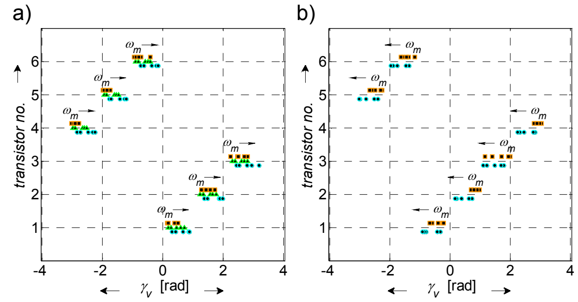

Fig.8. Registered values of the angle γ_v during the inverter transistor faults at the angular motor speed: ω_m>0 (a) and ω_m<0 (b)

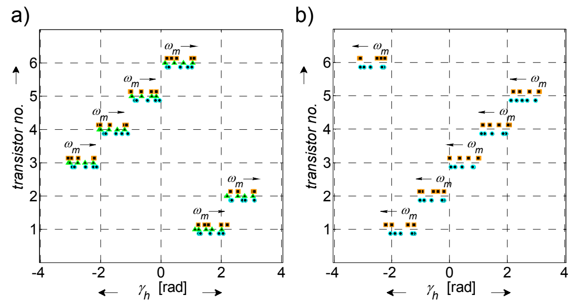

Fig.9. Registered values of the angle γ_h during the inverter transistor faults at the angular motor speed: ω_m>0 (a) and ω_m<0 (b)

As previously mentioned, a high effectiveness of the proposed fault diagnostic method is obtained due to the on-line membership functions C_k parameters adjustment, which is especially important in case of the diagnosis based on local maximum of $\hat{\psi}_r$. As an example, if the transistor T_1 fault occurs under an operation at the nominal speed of the drive, a lack of the parameters adaptation of the membership functions C_k provides the false alarms of the transistor T_2 failure (see Fig. 9a) or the transistor T_6 fault, if the motor operates at low speed (see Fig. 9b).

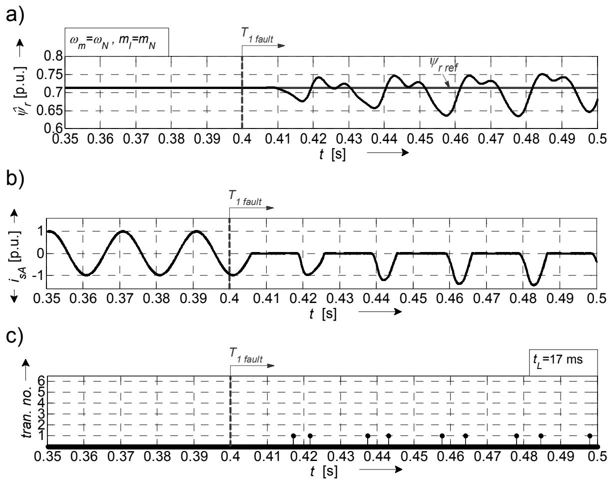

Fig.10. Reference $\psi_{r\ ref}$ and absolute value of the estimated rotor flux $\hat{\psi}_r$ (a) current in the faulty inverter phase i_{sA} (b) and output signal of the fault diagnostic system *tran. no.* (c) in case of T_1 fault

In Fig. 10-12 some simulation results related to transients of an absolute value of the estimated rotor flux $\hat{\psi}_r$, a current i_s in the faulty phase and an output signal of the fault diagnostic system *tran. no.* are presented. Additionally, a fault localization time t_L is indicated. At t=0.4s transistor failures were simulated under a steady state drive performance ω_m=const, m_l=const.

In accordance with Fig. 10b and 11b the open-circuit fault of the transistor T_1 and T_2 was simulated during their non conducting states. Moreover, in Fig. 12 the fault of T_3 was simulated during T_3 transistor conducting state, under low-speed drive operation and the load torque m_l=0.5m_N.

The simulation results prove an effectiveness of the proposed diagnostic method under wide motor speed range and whole range of the machine load torque. As can be seen, T_1 failure diagnosis took 17ms. When T_2 fault was simulated, the time t_L=18ms but in case of T_3 failure the fault localization time t_L=23ms. As can be noticed, the time t_L, that is required to fault diagnosis, is shorter than one stator current period, regardless of a transistor state during fault appearance.

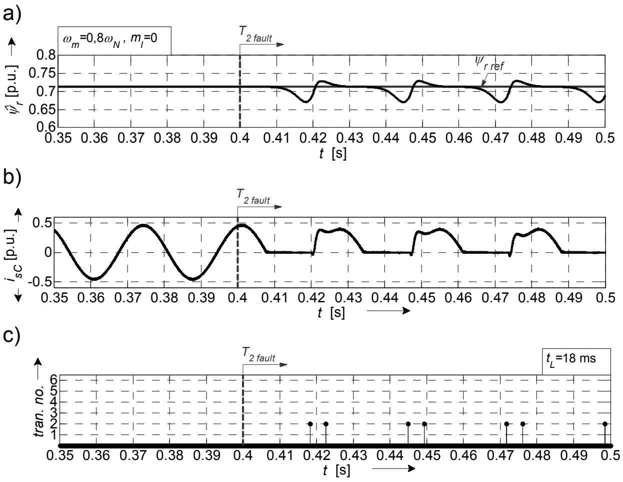

Fig.11. Reference $\psi_{r\ ref}$ and absolute value of the estimated rotor flux $\hat{\psi}_r$ (a) current in the faulty inverter phase i_{sC} (b) and output signal of the fault diagnostic system *tran. no.* (c) in case of T_2 fault

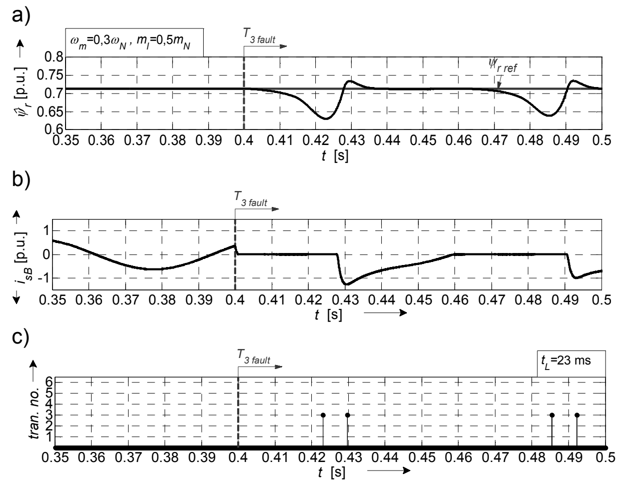

Fig.12. Reference $\psi_{r\ ref}$ and absolute value of the estimated rotor flux $\hat{\psi}_r$ (a) current in the faulty inverter phase i_{sB} (b) and output signal of the fault diagnostic system *tran. no.* (c) in case of T_3 fault

Conclusions

The novel fuzzy-logic-based approach to an inverter open-circuit transistor faults diagnosis in *DRFOC* induction motor drive was presented in this paper. A high effectiveness of the method was obtain by applying the on-line fuzzy system parameters adaptation according to changes of a drive speed. Due to the sequential scheme of the diagnostic system, computational diagnostic system requirements were minimized and a power system consumption is decreased. Additionally, the proposed diagnostic technique does not require extra sensors to realize the inverter open-switch fault diagnostic procedure. Transistor fault localization time is shorter than one stator current period.

This research work was supported by National Science Centre (Poland) under project DEC-2013/09/B/ST7/04199

LITERATURA

[1] Yang S., Xiang D., Bryant P., Ran L., Tavner P., Condition monitoring for device reliability in power electronic converters: a review, *IEEE Trans. on Power Electronics*, 25 (2010), 2734-2752

[2] Rodriguez M.A.; Claudio A.; Theilliol, D., Vela L.G., A New Fault Detection Technique for IGBT Based on Gate Voltage Monitoring, *Power Electronics Specialists Conference IEEE*, (2007), 1001-1005

[3] Araujo Ribeiro R.L., Jacobina C.B., Cabral da Silva E.R., Lima A.M.N., Fault detection of open-switch damage in voltage-fed PWM motor drive systems, *IEEE Trans. Power Electronics*, 18, (2004), n.2, 439-446

[4] Trabelsi M., Boussak M., Mestre P., Gossa M., An improved diagnosis technique for IGBTs open-circuit fault in PWM-VSI-fed induction motor drive, *IEEE Int. Symp. Industrial Electronics*, (2011), 2111-2117

[5] Lee Choi C,W., Design and evaluation of voltage measurement based sectoral diagnosis method for inverter open switch faults of permanent magnet synchronous motor drives, *IET–Electric Power Applications*, 6 (2012), 526-532

[6] Jung Shin-Myung, Park Jin-Sik, Kim Hyoung-Suk, Kim Hag-Wone, Youn Myung-Joong, Simple switch open fault detection method of voltage source inverter, *IEEE Energy Conversion Congress and Exposition*, (2009), 3175-3181

[7] Freire N.M.A., Estima J.O., Cardoso A.J.M., A voltage-based approach for open-circuit fault diagnosis in voltage-fed SVM motor drives without extra hardware, *XXth International Conference on Electrical Machines*, (2012), 2378-2383

[8] Mendes A.M.S., Cardoso A.J.M., Voltage source inverter fault diagnosis in variable speed AC drives, by the average current Park's vector approach, *Int. Conf. on Electr. Mach. and Drives*, (1999), 704-706

[9] Sobański P., Orłowska-Kowalska T., Metoda diagnostyki uszkodzenia typu przerwa łącznika IGBT falownika napięcia w układzie wektorowego sterowania silnikiem indukcyjnym, *Przegląd Elektrotechniczny,* 89 (2013), nr 6, 159-163

[10] Sobański P., Orłowska-Kowalska T., Wpływ uszkodzenia tranzystora IGBT falownika napięcia na przebiegi zmiennych stanu silnika indukcyjnego ze sterowaniem wektorowym, *Przegląd Elektrotechniczny,* 89 (2013), nr 2b, 62-165

[11] Mochan N., Advanced Electric Drives: Analysis, Control and Modeling Using Simulink, *MNPERE*, (2001)

[12] Orlowska–Kowalska T., Sensorless Induction Motor Drives, *Wroclaw University of Technology Press*, Wroclaw, (2003)

***Author**: Piotr Sobański, M.Sc., Wrocław University of Technology, Institute of Electrical Machines, Drives and Measurements, ul. Wybrzeże Wyspiańskiego 27, 57-370 Wrocław, piotr.sobanski@pwr.wroc.pl*